Revista Brasileira de Ciência do Solo

Division – Soil in Space and Time | Commission – Soil Survey and Classification

Non-allophanic Andosols of Trindade Island, south Atlantic: a new soil order in Brazil

Ana Carolina Campos Mateus[(1)], Angélica Fortes Drummond Chicarino Varajão[(1)], Fábio Soares de Oliveira[(2)*], Sabine Petit[(3)] and Carlos Ernesto Gonçalves Reynaud Schaefer[(4)]

[(1)] Universidade Federal de Ouro Preto, Departamento de Geologia, Programa de Pós-Graduação em Evolução Crustal e Recursos Naturais, Ouro Preto, Minas Gerais, Brasil.
[(2)] Universidade Federal de Minas Gerais, Instituto de Geociências, Departamento de Geografia, Belo Horizonte, Minas Gerais, Brasil.
[(3)] Université de Poitiers, Institut de Chimie des Mileux et Materiaux de Poitiers (IC2MP), Poitiers, França.
[(4)] Universidade Federal de Viçosa, Departamento de Solos, Viçosa, Minas Gerais, Brasil.

ABSTRACT: The pedological studies carried out so far in Trindade Island (TI) have obtained patchy evidences of allophane, without detailed mineralogical and micromorphological studies to confirm the occurrence of Andosols in TI. Therefore, in this study, the mineralogical, micromorphological, physical and chemical characterization of four soil profiles from Vulcão do Paredão (P1) and Morro Vermelho formations (P2, P3, and P4) were carried on the latest volcanic events in Brazil from Trindade Island (TI) with the aim of to evaluate the presence of Andosols in this oceanic island. Profiles P1 and P2 are developed on pyroclastic bombs, and show, respectively, A-Bi- C and decapitated A-C horizons, whereas P3 and P4 are developed on lapillitic and bomb pyroclasts, show A-C horizons. The soil profiles have a reddish and brownish clayey matrix, are highly friable and show a plastic consistency. Their microstructures are granular, single grain and intergrain microaggregate, in which aggregates display an undifferentiated b-fabric. The mineralogical constituents of the bulk fraction are biotite, hematite, magnetite, ilmenite, pyroxene, olivine, halloysite, goethite, anatase, and rutile. The clay fraction is marked by the presence of halloysite, ferrihydrite, and little amounts of allophane. All soils presented andic properties and can be classified as non-allophanic Andosols. In addition, micromorphological features closely resemble those reported in Andosols from other volcanic islands from elsewhere. The predominance of halloysite in the clay fraction formed by alteration of sideromelane, suggests that allophane would be an intermediate phase of this rapid transformation favored by the wet climate conditions of the highest parts of TI.

Keywords: volcanic island, Andic properties, Andisols, halloysite.

*** Corresponding author:**
E-mail: fabiosolos@gmail.com

Received: January 27, 2020
Approved: March 17, 2020

How to cite: Mateus ACC, Varajão AFDC, Oliveira FS, Petit S, Schaefer CEGR. Non-allophanic Andosols of Trindade Island, south Atlantic: a new soil order in Brazil. Rev Bras Cienc Solo. 2020;44:e0200007.
https://doi.org/10.36783/18069657rbcs20200007

INTRODUCTION

The soils formed from tephras or pyroclastic materials are known as Andisols (Soil Survey Staff, 2014), Andosols (IUSS Working Group WRB, 2015), and Kurobokudo (USCSJ, 2002). There are also some Andosols formed from non-tephritic materials, such as volcanic and sedimentary rocks, mixed materials of tephra and loess, etc. (Shoji et al., 1993). The Andosols are characterized by the presence of allophane or Al, Si, and humus compounds (Shoji et al., 1993). However, Shoji and Ono (1978) reported the occurrence of non-allophanic Andosols with Al/Fe humus characterized as Allophanic Andosols (Shoji et al., 1985). According to Soil Survey Staff (2014) an Andosol soil must have andic properties in at least 60 % of its profile. The andic properties of a soil are generally acquired during weathering of tephra or other parent materials which contain significant volcanic glass, leading to the formation of amorphous material as allophane, imogolite, ferrihydrite, or metal-humus complexes. The presence of amorphous materials is inferred from ammonium oxalate extraction of aluminum, iron, and silica (Soil Survey Staff, 2014). In the field, the andic soil properties may be inferred by using 1N sodium fluoride (NaF) (Soil Survey Staff, 2014). However, this test may not be specific for allophane as it may also reacts with A1 in Al-humus complexes (Parfitt, 1990).

The volcanic glass content is the percent of volcanic glass (by grain count) in the coarse silt and sand (0.02 to 2.0 mm) fraction (Soil Survey Staff, 2014). In addition, the pH(H_2O) >5, low content of organic matter, and base-rich volcanic ash favor the formation of allophane (Dahlgren et al., 1993).

According to Soil Survey Staff (2010), the Andosols cover approximately 0.8 % of the Earth's surface, and approximately 60 % of volcanic ash soils occur in tropical countries such as Colombia (Espinosa and Sanabria, 2015), Central México (Sedov et al., 2003), India (Caner et al., 2000), New Zealand (Neall, 1977). The remaining 40 % occur in cooler climate regions and are derived from various types of volcanic rocks, such as andesite, dacite, volcanic ash, basalt, and ignimbrite, distributed in different countries: Chile (Bertrand et al., 2008), Argentina (Candan and Broquen, 2009), Italy (Vingiani et al., 2014, 2018), France (Grison et al., 2015), Germany (Rennert et al., 2014), Georgia (Urushadze et al., 2011), Turkey (Kiliç et al., 2018), Kamchatka Peninsula of Russia (Litvinenko and Zakharikhina, 2009); and on non-volcanic rocks as gabbros, amphibolites, basic granulites, biotitic schists, amphibolitic phyllites: Spain (Bech-Borras et al., 1977; Garcia-Rodeja et al., 1987).

Particularly, in volcanic islands, there are a number of studies which focus on the identification of Andosols, such as in the Portuguese Azores and Cape Verde archipelago: São Miguel Island (Ricardo et al., 1977), Santa Maria and Graciosa (Madeira, 1980; Medina and Grilo, 1981), Terceira (Pinheiro, 1990), Madeira (Madeira et al., 1994), Faial and São Jorge (Madruga, 1995), Pico (Madeira et al., 1996; Pinheiro et al., 2001), Fogo (Faria, 1974), Sal (Diniz and Matos, 1993), São Nicolau (Diniz and Matos, 1999a), Brava (Diniz and Matos, 1999b) and São Vicente (Diniz and Matos, 1994); in Galápagos: Santa Cruz Island (Sedov et al., 2010); França: Reunion Island; Espanha: Canárias Island (Fernandez-Calilas et al., 1975); Japan (Adjadeh and Inoue, 1999), Indonesia (Devnita, 2012; Hikmatullah, 2008); Hawaiian Islands, Philippine Islands, Aleutas Islands and Solomon Islands.

In Brazil, studies showing the occurrence of Andosols are rare and Schaefer et al. (2017) were the first to postulate their presence on the oceanic island. Dümig et al. (2008) were the first to detect non-allophanic Andosols in South America outside the radius of influence of the recent volcanism of the Andes region. These Andosols were described in the northeastern of Rio Grande do Sul State and were developed from rhyodacite (Jurassic – Cretaceous volcanism).

Trindade Island (TI) is located in the mid-Atlantic with a surface of 13 km² and formed mostly by extrusive volcanic material and/or hyperabissal sodium-alkaline lava of Quaternary age (Almeida, 2002, 2006). Previously, Clemente et al. (2009) observed evidence of soils with andic properties and described a material similar to allophane at the base of a highland soil profile on tuffs, at the same location of the P1 of the present study. In soils developed from phonolitic and basic rocks of TI, Sá (2010) found pH values in NaF above 9.4, suggesting the presence minerals with a low degree of crystallinity, possibly allophane (Fields and Perrot, 1966; Brydon and Day, 1970). Consistently, phosphate retention values equal to or greater than 25 % and [Al (oxalate) + ½ Fe (oxalate)] > 0.4 were also observed (Sá, 2010). Clemente (2006) and Machado (2016) verified the presence of volcanic glass in a thin section in soils of TI, but a quantitative study was not performed, so they could not be clearly classified as Andosols.

Thus, the pedological studies carried out so far in TI have obtained patchy evidence of allophane, without detailed mineralogical and micromorphological studies to confirm the occurrence of Andosols in TI. To fill this gap, the present study aims to develop a combined mineralogical, micromorphological, physical, and chemical characterization of selected soils developed on TI pyroclasts to evaluate the presence of Andosols (Figure 1a) and, assess the pedo-environmental condition of their occurrence.

MATERIALS AND METHODS

Sample collected

Soil, rocks, and saprolites samples from four profiles were collected, one in the Vulcão do Paredão formation (VP) and three in the Morro Vermelho formation (MV) (Table 1). The contact sections between rocks and their respective alterites (iso and alloalterite) and solum (pedogenetic horizons) were described and sampled in the field according to the standard guidelines (Santos et al., 2015).

The descriptions highlighted the main morphological variations at macroscopic scale, combined with the use of a magnifying glass (20X). Aspects such as color (Munsell, 2009), texture, and structure were described (Table 1).

Physical and chemical analyses

The physical and chemical analyses were performed in the Laboratory of Soil Analysis of the Federal University of Viçosa, following international standard procedures (Teixeira et al., 2017). The contents of sand, silt, and clay fractions were measured after slow agitation (16 h) using chemical dispersion with 10 mL of NaOH 1 mol $L^{-1,}$ and the proportions of each fraction were plotted in the triangular diagram to obtain the textural class. Coarse and fine sand were separated by sieving and, silt and clay were determined by the pipette method.

The bulk density was performed by volumetric cylinder method (Almeida et al., 2017). The samples collected in the field in metallic cylinders of 100 g cm^{-3} and were dried at 105 °C for 48 h, to obtain the soil density.

The quantification of volcanic glass was obtained from the coarse silt to sand fractions by separation by a magnifying glass Nikon C-POL.

The pH was measured in H_2O (soil: solution 1:2.5) and in NaF (Pansu and Gautheyrou, 2006); the Melich-P concentrations were reported in mg dm^{-3} (Defelipo and Ribeiro, 1981); the exchangeable contents of K, Ca, Mg, and Al in $cmol_c$ dm^{-3}, allowed to sum of exchangeable bases (SB), the effective cation exchange capacity CEC (t), and total CEC (T) in $cmol_c$ dm^{-3}, base saturation (V) and aluminum saturation (m) in %. The

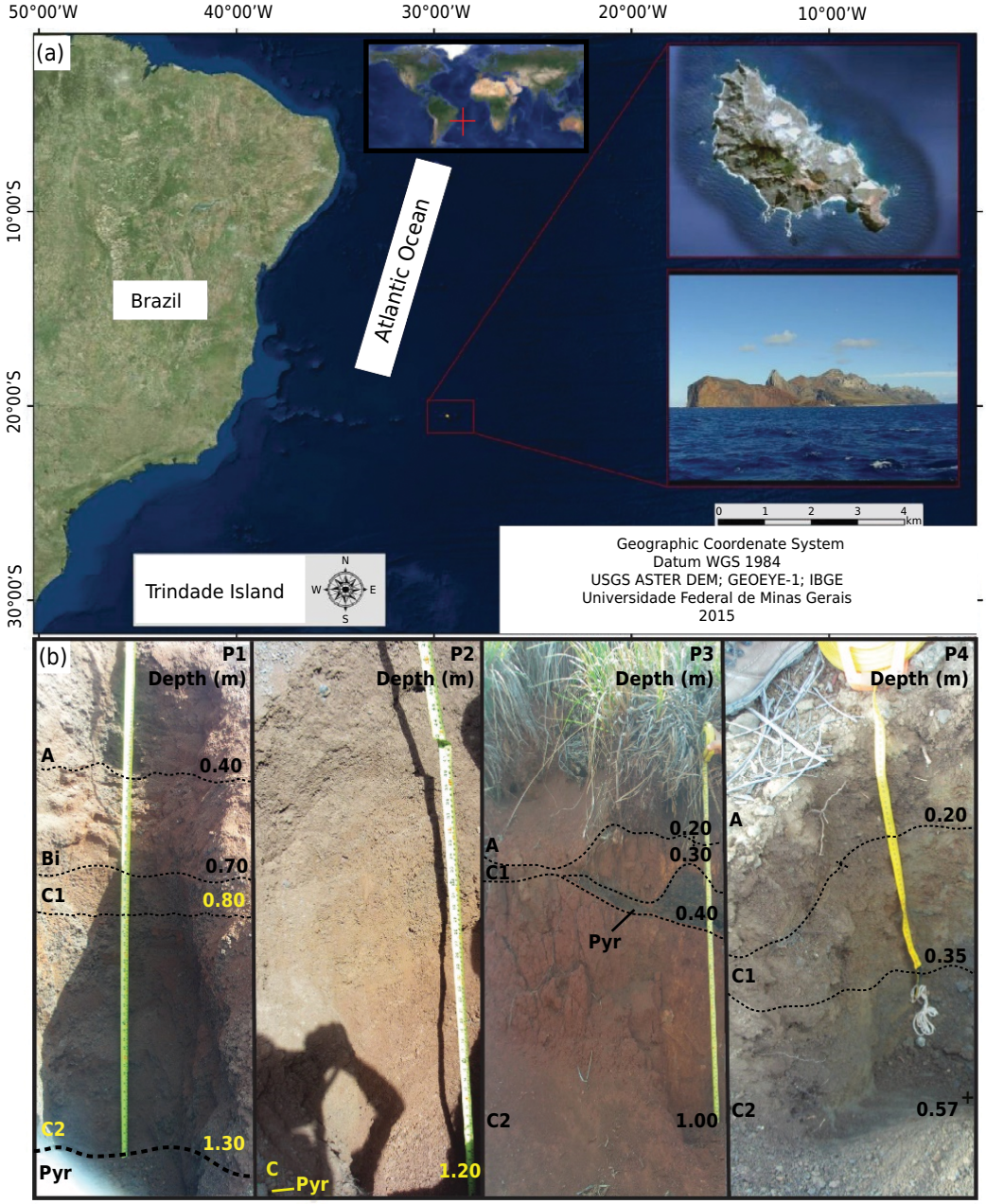

Figure 1. Location of Trindade Island in the South Atlantic Ocean (a). Elaborated by Mariana Rezende Machado. Location of profiles in VP (P1) and MV formations (P2, P3, and P4) and description of pedological horizons. Modified of Mateus et al. (2018) (b). A: A horizon; Bi: Bi horizon; C1: C1 horizon; C2: C2 horizon; Pyr: pyroclasts.

organic matter (OM) content was determined by the Walkley-Black method, while the total organic carbon (TOC) content was estimated, in g kg^{-1}, by the equation (OM × 1.724). The P remaining (Prem) was calculated according to Alvarez et al. (2000) and P retention percentage (PR) as follows: P in the blank minus P in the equilibration solution (Prem).

Mineralogical analyses

The identification of the mineralogical phases was performed by X-ray diffractometry (XRD) in the fine-earth fraction and the clay fraction (<2 µm). The clay samples were saturated with Ca^{2+}, deferrified with sodium dithionite-citrate-bicarbonate (DCB) according to the methodology of Mehra and Jackson (1960), treated with formamide and dehydrated at 110 °C for 6 h. The analyses were carried out in a Panalytical Empyrean

Table 1. Physical properties of Trindade Island soils

Hor.	Layer	Particle size							Color		Consistence		Plast.	Structure	BD	VG
		< 2mm				Silt/ Clay	Textural class	2 mm>x>2 mm	Wet	Dry	Dry	Moist				
		Coarse sand	Fine sand	Silt	Clay											
	m	g kg^{-1}						%							Mg m^{-3}	%
								P1- VP								
A	0.00-0.40	26.0	111.0	384.0	478.0	0.80	Clay	52.1	7.5YR 3/2 Dark brown	7.5YR 3/2 Dark brown	L	FR	SP	SBK weak medium to coarse	7.5*10^{7}	5.4
Bi[1]/Bw[2]	0.40-0.70	12.0	78.0	360.0	549.0	0.65	Clay	45.0	7.5YR 3/2 Dark brown	7.5YR 4/4 Brown	SH	FI	SP	PL weak mediun	9.3*10^{7}	5.0
C1	0.70-0.80	23.0	159.0	399.0	419.0	0.95	Clay	58.1	7.5YR 3/4 Dark brown	7.5YR 4/6 Strong brown	L	FR	SP	ABK weak fine	9.3*10^{7}	7.4
C2	0.80-1.30	68.0	180.0	358.0	394.0	0.91	Clay loam	60.6	7.5YR 3/2 Dark brown	7.5YR 4/6 Strong brown	L	VFR	SP	ABK weak fine	7.1*10^{7}	12.76
Pyr	1.30^{+}	-	-	-	-	-	-	-	5YR 4/3 Reddish brow	7.5YR 5/2 Brown	-	-	-	MA		
								P2- MV								
C	0.00-1.20	259.0	82.0	251.0	409.0	0.61	Clay	59.2	7.5YR 4/6 Strong brown	7.5YR 4/6 Strong brown	S	VFR	P	ABK weak fine to mediun	11.6*10^{7}	8.10
Pyr	1.20^{+}	-	-	-	-	-	-	-	5YR 4/3 Reddish brow	7.5YR 5/2 Brown	-	-	-	MA	-	-
								P3- MV								
A	0.00-0.20	35.0	67.0	323.0	575.0	0.56	Clay	42.6	7.5YR 3/2 Dark brown	7.5YR 3/2 Dark brown	L	L	SP	SGR	7.2*10^{7}	4.16
C1	0.20-0.30	51.0	74.0	298.0	577.0	0.51	Clay	42.3	7.5YR 4/4 Brown	7.5YR 4/4 Brown	VH	VFI	P	SBK moderate medium to fine	10.1*10^{7}	16.66
Pyr	0.30-0.40	-	-	-	-	-	-	-	5YR 4/3 Reddish brown	7.5YR 5/2 Brown	-	-	-	MA	-	
C2	0.40-1.00	50.0	22.0	247.0	681.0	0.36	Very clayey	31.9	5YR 3/3 Reddish Strong	7.5YR 3/4 Dark brown	H	VFI	P	SBK moderate medium to fine	9.6*10^{7}	3.50
								P4- MV								
A	0.00-0.20	120.0	66.0	497.0	316.0	1.57	Silt clay loam	68.3	10YR 4/3 Brown	10YR 5/3 Brown	S	FR	P	SGR ABK	7.1*10^{7}	5.9
C1	0.20-0.35	107.0	48.0	582.0	263.0	2.21	Silt	73.7	10YR 3/3 Strong Brown	10YR 5/3 Brown	S	FI	SP	ABK weak fine	13.8*10^{7}	0.59
C2	0.35-0.57^{+}	283.0	50.0	459.0	209.0	2.20	Silt loam	79.2	10YR 4/3 Brown	10YR 5/3 Brown	S	FR	SP	MA	-	0.66

Sand, silt, and clay were determined by Pipette method. Bulk density was determined by volumetric ring method. Hor.: horizon; Pyr: pyroclasts; BD: bulk density; VG: volcanic glass; L: loose; SH: slightly hard; S: soft; H: hard; FR: friable; FI: firm; VFR: very friable; VFI: very firm; SBK: subangular blocky; Pl: platy; ABK: angular blocky; MA: massive; SGR: single grain; SP: slightly plastic; P: plastic. 1: coding of horizon according to Brazilian Soil Classification System (Santos et al., 2018); 2: coding of horizon according to Soil Taxonomy (Soil Survey Staff, 2014).

(CuKα, 45 KV and 40 mA) and in the Philips X ' Pert Pro Diffraction (CuKα, 40 KV, 40 mA) diffractometers. The scanning interval for the fine-earth fraction analysis was from 2 to 70 °, with a step of 0.02° (2θ min^{-1}); and for the analysis of the clay fraction from 2 to 35°, with step 0.4° (2θ min^{-1}). The diffractograms were interpreted by using the X'Pert HighScore Plus software and through the literature references (Brown and Brindley, 1980).

Infrared spectroscopy was used to assist the mineralogical analyses. The analyses were performed in the IC2MP Institute, University of Poitiers using Fourrier transform spectrometers (Thermo Nicolet, Nexus 5700 series) for analyses of the bulk and clay fractions. The pressed discs were made with 1 mg of sample and 150 mg of KBr, which were analyzed with natural moisture and then dehydrated at 120 °C for 20 h and at 200 °C for 4 h to remove absorbed water. The mid-infrared spectra (4000-400 cm^{-1}) were obtained using a source of white light, beamsplitter KBr, resolution of 4 cm^{-1}, the optical velocity of 0.4747 cm s^{-1}, and 100 scans. Clay fraction images were obtained by a Transmission Electron Microscope (TEM) JEOL 2011 Bruker Esprit in the CinaM-CNRS, Aix Marseille University. The suspended clay was deposited on carbon coated Formvar film Cu grids.

Micromorphological and microchemical analyses

Thin sections of soils and rocks previously impregnated were described in a Zeiss microscope fitted with a digital camera. The micromorphological description of soils was based on Stoops (2003) and (Stoops et al., 2018).

The microchemical analyses were performed with electron microprobe JEOL JXA-8230 at the Microanalysis Laboratory of Geology Department/Federal University of Ouro Preto. The acceleration and current conditions were 15 kV and 20 nA, and corrections of the common ZAF matrix were applied. Counting times on the peaks/background were 10/5 s for all elements (Si, Al, Fe, Ca, Na, and K), except for Ba (30/15 s). The point-source analyses were calibrated with quartz-TAP, coridon-TAP, almandine- LIFH, augite- PETJ, anorthoclase- TAPH, microcline- PETL, and barite- PETH. The FeO was considered as the amount of total iron obtained through the microprobe.

Selective extraction and allophane and ferrihydrite estimation

Selective extraction of Al, Si, and Fe was performed with sodium pyrophosphate (Blakemore et al., 1981), ammonium oxalate (MacKeague and Day, 1966), and sodium dithionite-citrate-bicarbonate (Mehra and Jackson, 1960; Holmgreen, 1967). The elemental contents were determinate by ICP-OES, for quantification of amorphous and crystalline phases.

The A1:Si ratio of the allophane was calculated from [A1(o)-Al(p)]/Si(o) and the amount of allophane in the sample was estimated by multiplying of Si(o) by the factor proposed by Parfitt (1990): for Al:Si atomic ratios close to 1.0, 1.5, 2.0, 2.5, 3.0, 3.5, is multiplied Si(o) by the factors 5, 6, 7, 10, 12, 16, respectively. Ferrihydrite content was determined by multiplying Fe(o) values by l.7 (Parfitt and Childs, 1988).

RESULTS

Physical and chemical properties

Table 1 shows the macromorphological and physical characteristics of the four soil profiles. The profile P1 is 1.30 m thick and is located at an elevation of 460 m, with A, Bi, C1, and C2 horizons and developed from pyroclastic bombs (Figure 1b, Table 1). Profile 2 (P2), is 1.20 m thick, located at 351 m on deposit of pyroclastic bombs, and has lost most of its A horizon; P3, at an elevation of 258 m, is approximately 1.00 m thick and shows A, C1 and C2 horizons, with 0.10 m layer of lapillitic pyroclasts between C1 and C2; P4 has a thickness of 0.57 m, located at an elevation of 72 m, with a sequence of A, C1, and C2 horizons. Bulk density is low (<0.90 g cm^{-3}), consistently with soils developed from volcanic ash (Soil Survey Staff, 2014).

All soils have high amounts of volcanic glass in the coarse sand fraction of C horizons of P1, P2, and P3 (12.76, 8.10, and 20.96 %), and lower amounts in the A horizon of P4 (4.16 %)

(Table 1, Figure 2). In P1, the glass is stained (reddish brown to yellowish), showing alteration to palagonite. However, this alteration is only partial in P2, P3, and P4 (Figure 2).

The bases saturation of P1 (VP) is lower than P2, P3, and P4 (MV) decreasing to the A horizon (Table 2). Profile 1 (P1) is located at the highest altitude; hence it is exposed to more intense weathering, which promotes greater leaching of K^+, Na^+, Ca^{2+}, and Mg^{2+}, resulting in lower pH(H_20) –between 4.82 and 6.01. The pH in NaF is greater than 9.5 in all horizons, except A and C2 of P3. The sum of exchangeable bases (EB), effective CEC [CEC(t)] and potential CEC [CEC(T)] are high, which suggests little weathered young soils. A slight increase of EB is seen in the A horizon highlighting the influence of organic surface. The base saturation (V) is lower than 50 % in A, Bi, and C1 of P1, and above 50 % in all others (P2, P3, and P4) (Table 2). This characterizes the P1 as a dystrophic and the other profiles as eutrophic. The content of exchangeable aluminum (Al^{3+}) is high in A, Bi, C1 horizon of P1, with a marked value in A horizon (4.2 $cmol_c$ kg^{-1}). In all other soils, the content of Al^{3+} is null. The available phosphorous showed similar values to soils on tuffs described by Clemente et al. (2009); the phosphorous may be attributed to sideromelane (0.8 % in pyroclasts of P2 and P3), and 2.3 % in palagonitized sideromelane of P1 (Mateus et al., accepted article). The sodium saturation in the C2 horizon of P1 and P4 represents a solodic character (sodium saturation between 6 and 15 %). The phosphate retention (PR) is high in all horizons with values between 65 and 97 %; in contrast, the total organic carbon contents (TOC) are low (Table 2).

Selective extraction of Si, Al, and Fe

The table 3 shows selective extraction for the four soil profiles. For all profiles the values of Al(o) are higher than Al(d), indicating higher concentration of Al in amorphous phases.

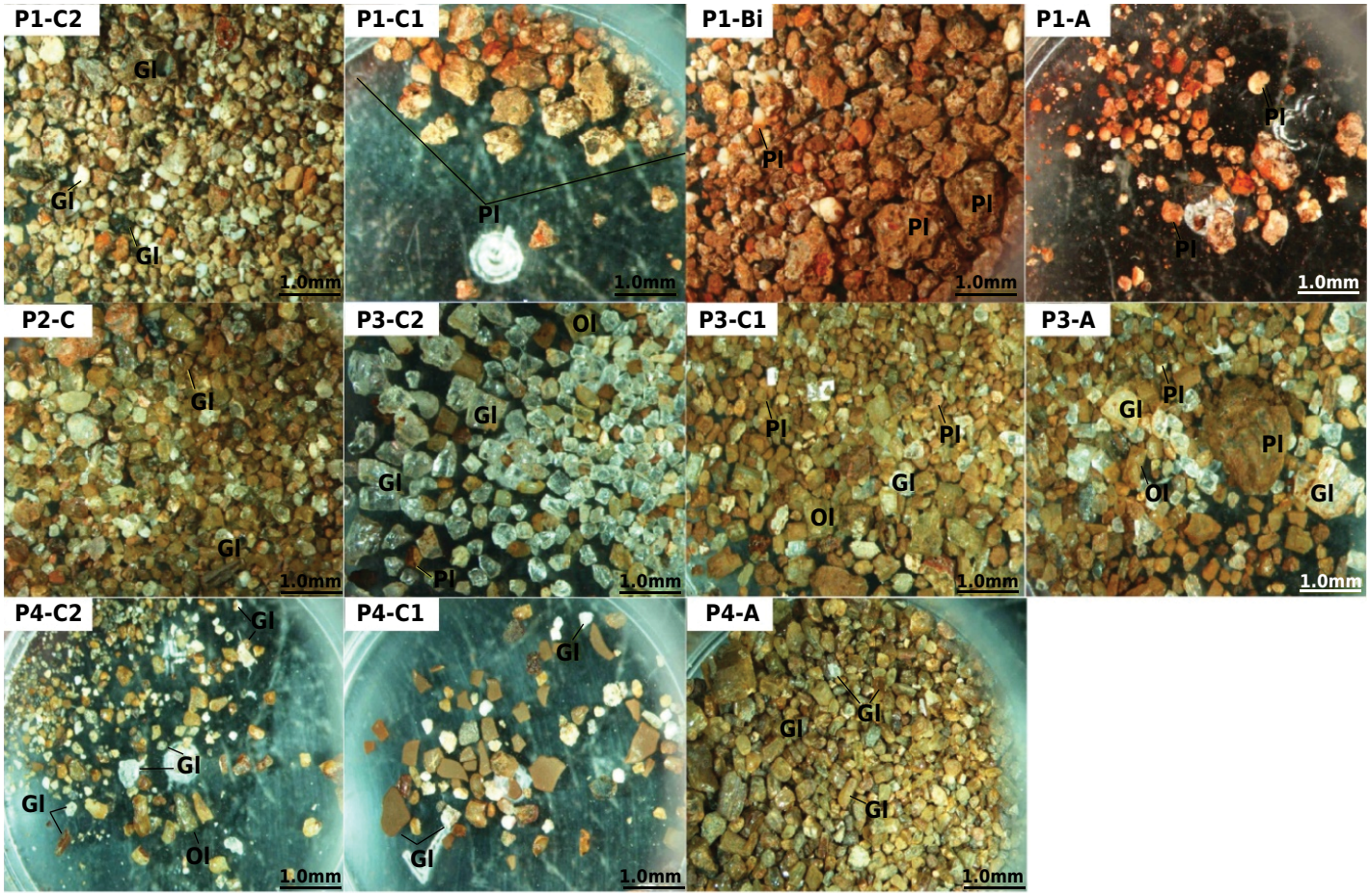

Figure 2. Glass volcanic of light-yellow color in the coarse sand of P1, P2, P3, and P4. It is noted than the amount of palagonitized volcanic glass increases in all horizons of P1 and, in C1 and A of P3. Gl: volcanic glass; Pl: palagonite: Ol: olivine.

The iron and silicon contents show an inverse behavior. Lower Fe(o) and Si(o) amounts than F(d) and Si(d), suggest a predominance of well- crystalline minerals in all profiles.

The soils are more enriched in Al–humus complexes than in Fe and Si–humus complexes. In particular, the values of Al–humus complexes are higher in P2, P3, and P4.

The relationship of Al(p) and Al(o) are between 0.37 and 1.22, with greater values in P3 (0.84, 0.72, and 1.22) and lower in P4 (0.37 and 0.46).

The ratio [A1(o)-Al(p)]/Si(o) values are lower in P2 (0.48) and greater in P4 (2.51), indicating a lower (3.56 g kg^{-1}= 0.36 %) and higher (31.85 g kg^{-1}= 3.19 %) contribution of allophane, respectively. The amounts of ferrihydrite are high in all profiles, with higher value in C1 of P4 (135.66 g kg^{-1} = 13.57 %).

Table 2. Chemical properties of Trindade Island soils

Pedon	Hor.	Layer	pH			P^{5+}	K^+	Na^+	Ca^{2+}	Mg^{2+}	Al^{3+}	H^++Al^{3+}	EB	CEC(t)	CEC(T)	V	m	ISNa	TOC	Prem	PR
			H_2O	HCl	NaF																
		m				$cmol_c\ dm^{-3}$										%			$g\ kg^{-1}$	$mg\ L^{-1}$	%
P1	A	0.00-0.40	4.82	3.80	9.67	0.15	0.10	0.86	1.16	1.52	4.20	11.60	3.63	7.83	15.23	23.8	53.6	5.63	2.15	2.20	96.33
	Bi[1]/Bw[2]	0.40-0.70	5.06	3.97	9.89	0.06	0.16	0.71	0.95	1.79	1.90	9.60	3.61	5.51	13.21	27.3	34.5	5.41	1.45	2.60	95.66
	C1	0.70-0.80	4.99	7.29	9.69	0.07	0.17	0.71	1.04	2.94	2.50	9.70	4.86	7.36	14.56	33.4	34.0	4.91	0.00	2.6	95.66
	C2	0.80-1.30	6.01	4.75	9.75	0.20	0.20	2.80	1.39	7.87	0.10	6.30	12.26	12.36	18.56	66.1	0.8	15.08	0.00	3.80	93.66
P2	C	0.00-1.20	7.51	6.17	9.54	11.82	0.40	0.71	12.07	7.95	0.0	2.30	21.14	21.14	23.44	90.2	0.0	3.05	7.19	20.10	66.55
P3	A	0.00-0.20	6.72	5.43	9.24	0.59	1.54	1.63	7.85	11.05	0.0	5.90	22.07	22.07	27.97	78.9	0.0	5.82	18.03	8.90	85.16
	C1	0.20-0.30	7.37	5.99	9.83	0.43	1.23	0.71	9.08	7.84	0.0	2.80	18.87	18.87	21.67	87.1	0.0	3.30	12.99	7.80	87.00
	C2	0.30-1.00	7.73	6.13	9.43	0.42	1.31	1.19	9.23	9.70	0.0	2.30	21.43	21.43	23.73	90.3	0.0	5.03	0.69	6.50	89.16
P4	A	0.00-0.20	7.13	7.13	9.57	16.07	0.54	0.82	9.86	8.36	0.0	4.30	19.59	19.59	23.89	82.0	0.0	3.46	9.39	19.20	68.00
	C1	0.20-0.35	7.29	5.68	9.55	13.94	1.05	1.06	8.12	6.87	0.0	2.30	17.11	17.11	19.41	88.2	0.0	5.47	2.15	21.20	64.66
	C2	0.35-0.57+	7.45	-	9.77	12.23	1.18	1.28	7.32	6.62	0.0	2.30	16.40	16.40	18.70	87.7	0.0	6.84	2.15	20.60	65.66

pH(H_2O): pH in water-saturated soil paste (1:2.5); K^+ (Mehlich 1); Ca^{2+}, Mg^{2+}, and Al^{3+} (KCl 1 mol L^{-1}); H+Al (Calcium acetate 0.5 mol L^{-1} at pH 7.0); EB: exchangeable bases sum; CEC(t): effective cation exchange capacity; CEC(T): potential cation exchange capacity (at pH 7.0); V: bases saturation; m: aluminum saturation; ISNa: sodium saturation; TOC: total organic carbon (Yeomans and Bremner, 1988); Prem: P remaining; PR: P retention. [1] Coding of horizon according to Brazilian Soil Classification System (Santos et al., 2018); [2] Coding of horizon according to Soil Taxonomy (Soil Survey Staff, 2014).

Table 3. Selective dissolution and mineralogical properties of TI soils

Pedon	Hor.	Al(o)	Fe(o)	Si(o)	Al(d)	Fe(d)	Si(d)	Al(p)	Fe(p)	Si(p)	Aph[1]	Fh[2]	Al(o)+ 0.5Fe(o)	Al/Si[3]	Al(p)/ Al(o)	Fe(p)/ Fe(o)	Fe(o)/ Fe(d)
		$g\ kg^{-1}$												atomic ratio			
P1	A	11.31	21.1	2.23	6.36	108.5	5.85	7.08	0.43	0.29	15.59	35.87	21.86	1.89	0.62	0.02	0.19
	Bi[3]/Bw[4]	9.21	18.05	2.10	5.42	82.11	4.92	6.18	0.28	0.22	12.57	30.68	18.23	1.44	0.67	0.01	0.22
	C1	11.53	21.52	2.90	6.13	96.35	4.94	5.34	0.38	0.33	17.38	36.58	22.29	1.77	0.46	0.02	0.22
	C2	10.57	19.11	2.99	5.58	71.87	5.19	3.93	0.28	0.32	20.95	32.49	20.12	2.23	0.37	0.01	0.26
P2	C	8.40	20.18	3.56	6.17	70.86	9.56	6.90	0.56	0.60	3.56	21.88	18.49	0.41	0.82	0.02	0.28
P3	A	8.96	24.77	3.49	6.87	92.93	5.64	7.56	0.62	0.54	17.45	42.11	21.34	1.05	0.84	0.02	0.27
	C1	11.29	26.75	2.98	7.70	86.84	4.90	8.19	0.58	0.47	17.90	45.70	24.76	1.64	0.72	0.02	0.31
	C2	8.39	24.55	3.86	5.85	103.06	7.11	10.28	27.29	4.30	3.86	41.73	20.66	0.48	1.22	1.11	0.24
P4	A	12.10	19.96	3.18	5.29	25.39	7.61	6.05	0.86	0.69	31.85	33.93	22.08	2.52	0.50	0.04	0.79
	C1	11.40	20.75	4.17	6.17	23.32	9.02	6.38	0.62	0.76	29.19	135.66	21.77	2.05	0.56	0.03	0.89
	C2	10.80	17.47	3.99	5.49	19.03	9.50	11.79	0.58	0.79	19.94	29.70	19.53	0.74	1.09	0.03	0.92

[1] Allophane: Si(o) multiplied by a factor Parfitt (1990); [2] ferrihydrite: Fe(o) × 1.7; [3] (Al(o) -Al(p)/Si(o). [3] Coding of horizon according to Brazilian Soil Classification System (Santos et al., 2018); [4] Coding of horizon according to Soil Taxonomy (Soil Survey Staff, 2014). Hor.: horizon.

Micromorphology, mineralogical and microchemical properties

The pyroclasts (Figure 3a) show vesicular and amygdaloid structures and show sideromelane altered to palagonite. Mineralogically, they consist of biotite, hematite, magnetite, ilmenite, pyroxene (diopside and augite), olivine (forsterite), and zeolites (chabazite) (Mateus et al., 2020). The pedological horizons of all profiles have the same minerals in the fine-earth, in addition, goethite, anatase, and halloysite. Oligoclases and anorthoclases (Table 4; Figure 4) of 3.0 mm size occur in 2 % of the thin section in C2 and C1 (Figure 3j) from the P4 profile.

The C horizons show coarse material composed by dark brown very altered subangular fragments of vesicular pyroclasts (Figures 3b, 3g, and 3k), besides a reddish brown clayey micromass composed of fine biotite, halloysite, hematite, goethite, anatase, magnetite (Figures 5a, 5b, 5c, and 5d). Halloysite is the only clay mineral resulting from pyroclasts weathering (Figures 6a, 6b, 6c, and 6d), and shows a tubular habitus, annotated with the presence of granular hematite and acicular goethite (Figures 7a, 7c, 7e, and 7f). In particular, the infrared spectra of pyroclasts from P3 showed a less crystalized signature, probably sideromelane (Figure 6c).

The c/f related distribution is coarse monic in C horizons (Figure 3b), changing to chitonic and eunalic in Bi and A horizons, showing a single grain and intergrain microaggregate microstructure, respectively at the bottom and top of the profiles (A and Bi horizons), (Figures 3b, 3f, 3h, and 3i). In Bi and A horizons, the pyroclasts fragments are split into smaller fragments characterizing the transition from simple grain to intergrain microaggregate microstructure (Figures 3d, 3f, and 3i).

Table 4. Microchemical analyses in feldspars crystals in C2 horizon, P4

Region point	Crystal A				Crystal B			Crystal C		
	Edge	Edge	Edge	Interm.	Edge	core	Edge	Edge	Edge	Edge
	1	2	3	4	1	2	3	1	2	3
	%									
SiO_2	60.15	60.27	59.20	61.67	62.07	62.49	62.21	60.32	59.37	59.43
Al_2O_3	24.61	24.35	25.03	24.01	23.17	22.99	23.19	24.315	24.048	24.62
FeO	0.39	0.47	0.35	0.36	0.34	0.33	0.38	0.34	0.34	0.32
CaO	4.06	3.65	4.15	3.46	2.56	2.56	2.54	3.44	3.28	2.99
Na_2O	7.37	7.42	7.40	7.83	7.72	7.64	7.67	7.50	7.19	6.94
K_2O	1.72	1.81	1.51	2.09	2.71	3.14	2.84	1.96	2.16	2.60
BaO	0.00	0.00	0.00	0.00	0.00	0.00	0.00	0.00	0.00	0.00
Total	100.52	100.32	100.59	99.33	98.57	99.15	100.54	100.34	96.38	96.90
Si	2.72	2.74	2.70	2.76	2.80	2.81	2.80	2.74	2.74	2.73
Al	1.31	1.30	1.34	1.27	1.23	1.22	1.23	1.30	1.31	1.33
Fe	0.01	0.02	0.01	0.01	0.01	0.01	0.01	0.01	0.01	0.01
Ca	0.20	0.18	0.20	0.17	0.12	0.12	0.12	0.17	0.16	0.15
Na	0.65	0.65	0.65	0.68	0.68	0.67	0.67	0.66	0.64	0.62
K	0.10	0.10	0.09	0.12	0.16	0.18	0.16	0.11	0.13	0.15
Ba	0.00	0.00	0.00	0.00	0.00	0.00	0.00	0.00	0.00	0.00
Xca=Ano	20.9	19.0	21.5	17.2	13.0	12.7	12.8	17.8	17.4	16.0
Xna=Ab	68.6	69.8	69.3	70.4	70.7	68.7	70.1	70.1	69.0	67.4
XK=Or	10.5	11.2	9.3	12.4	16.3	18.6	17.1	12.1	13.6	16.6

Calculated according to Deer et al. (2013).

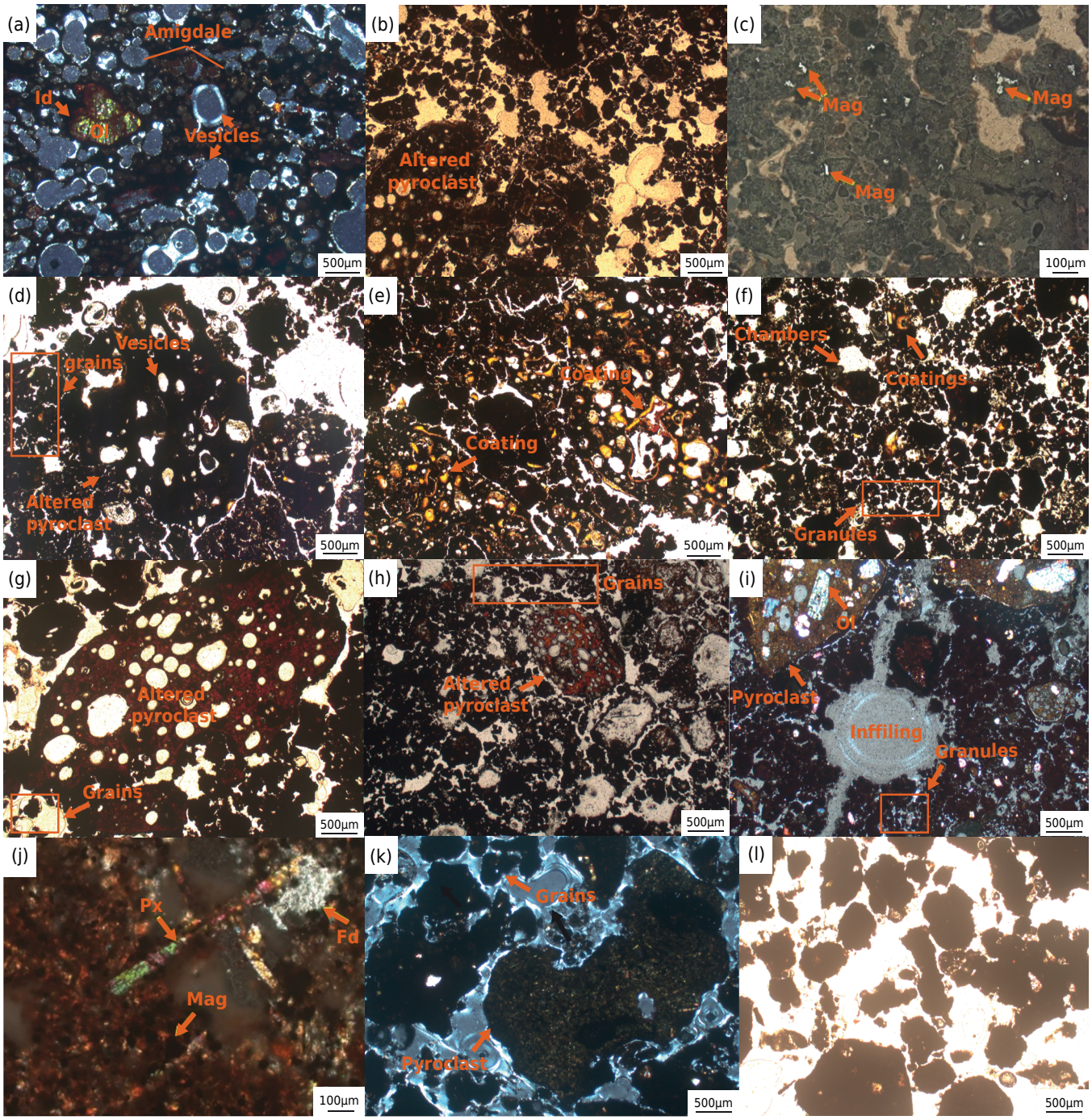

Figure 3. XPL photomicrograph of pyroclasts from P1 showing vesicles and olivine iddingsitized (a). PPL photomicrograph of C2 horizon from P1 showing altered vesicular pyroclasts and a simple grains microstructure evidenced by c/f related distribution is coarse monic (b). Reflected light photomicrograph of C1 horizon from P1 showing magnetite crystals in the clay matrix and pyroclast fragments (c). PPL photomicrograph of Bi horizon from P1 showing altered pyroclast fragments divided into smaller fragments (d). PPL photomicrograph of Bi horizon from P1 showing coatings of clay and c/f chitonic distribution (e). PPL photomicrograph of A horizon from P1 showing granular and intergrain microaggregate microstructures and coating of clay (f). PPL photomicrograph of C horizon from P2 showing pyroclast fragment with sideromelane totally palagonitized and grains of altered pyroclasts of 250mm (g). PPL photomicrograph of C2 horizon from P3 showing simple grains (h). XPL photomicrograph of A horizon from P3 showing pyroclast fragment with unaltered Ol, granules of clay aggregates with undifferentiated b-fabric and infilling (i). XPL photomicrograph of C2 horizon from P4 showing pyroclast fragment with pyroxenes, magnetites and feldspar (j). XPL photomicrograph of C1 horizon from P4 showing pyroclast fragment and aggregates of clay (k). PPL photomicrograph of A horizon from P4 showing granular microstructure (l). Ol: olivine; Id: iddingsite; Px: pyroxene; Mag: magnetite; Fd: feldspar; XPL: crossed polarized light; PPL: plane polarized light.

The typical granular microstructure also occurs in the A horizon (Figures 3f and 3l). The pyroclasts fragments and olivine and magnetite crystals decrease in size and quantities towards to the surface. At the bottom (C2 horizon), pyroclasts fragments of 15.0 mm

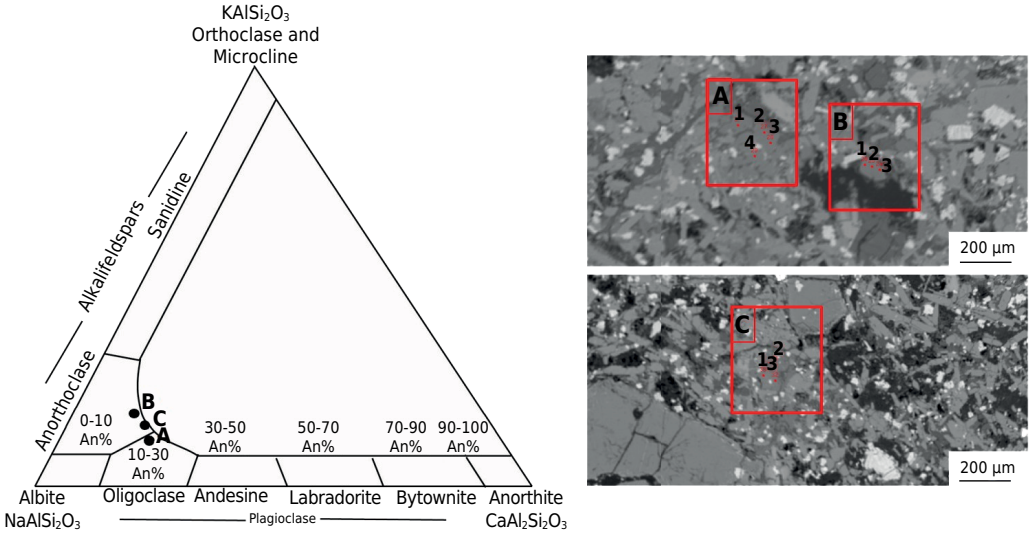

Figure 4. Feldspar diagram and SEM images of the C2 horizon. The plot of microchemical analyses in the diagram shows that the crystal A is an oligoclase and, B and C are anorthoclase.

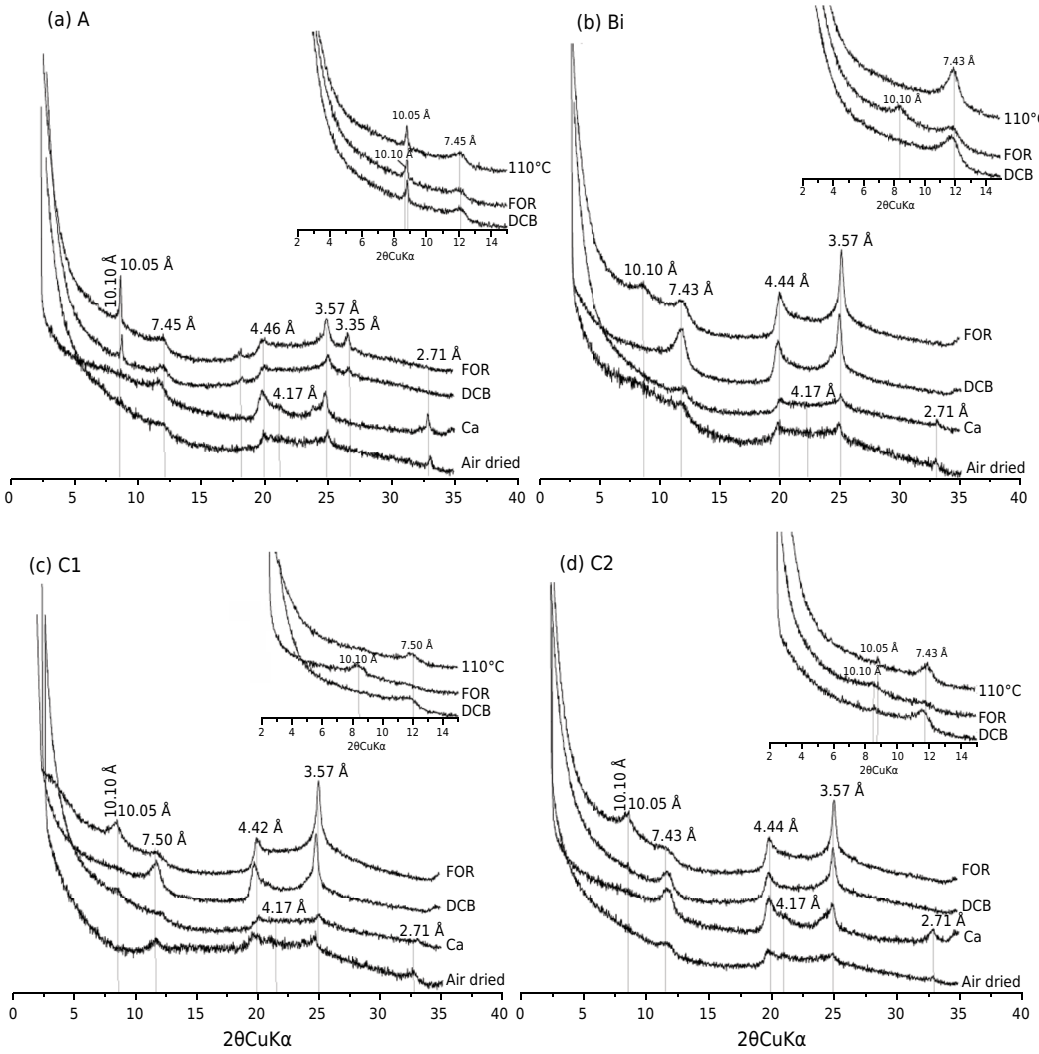

Figure 5. X-ray diffraction patterns of A (a), Bi (b), C1 (c), and C2 (d) horizons from P1 of clay fraction air dried, saturated with Ca^{2+} (Ca), deferrified with sodium dithionite-citrate-bicarbonate (DCB) and saturated with formamide (FOR). Biotite: 10.10 Å; 3.35 Å; Halloysite: 10.05 Å; 7.45 Å, 4.46 Å, 3.57 Å; Hematite: 2.71 Å.

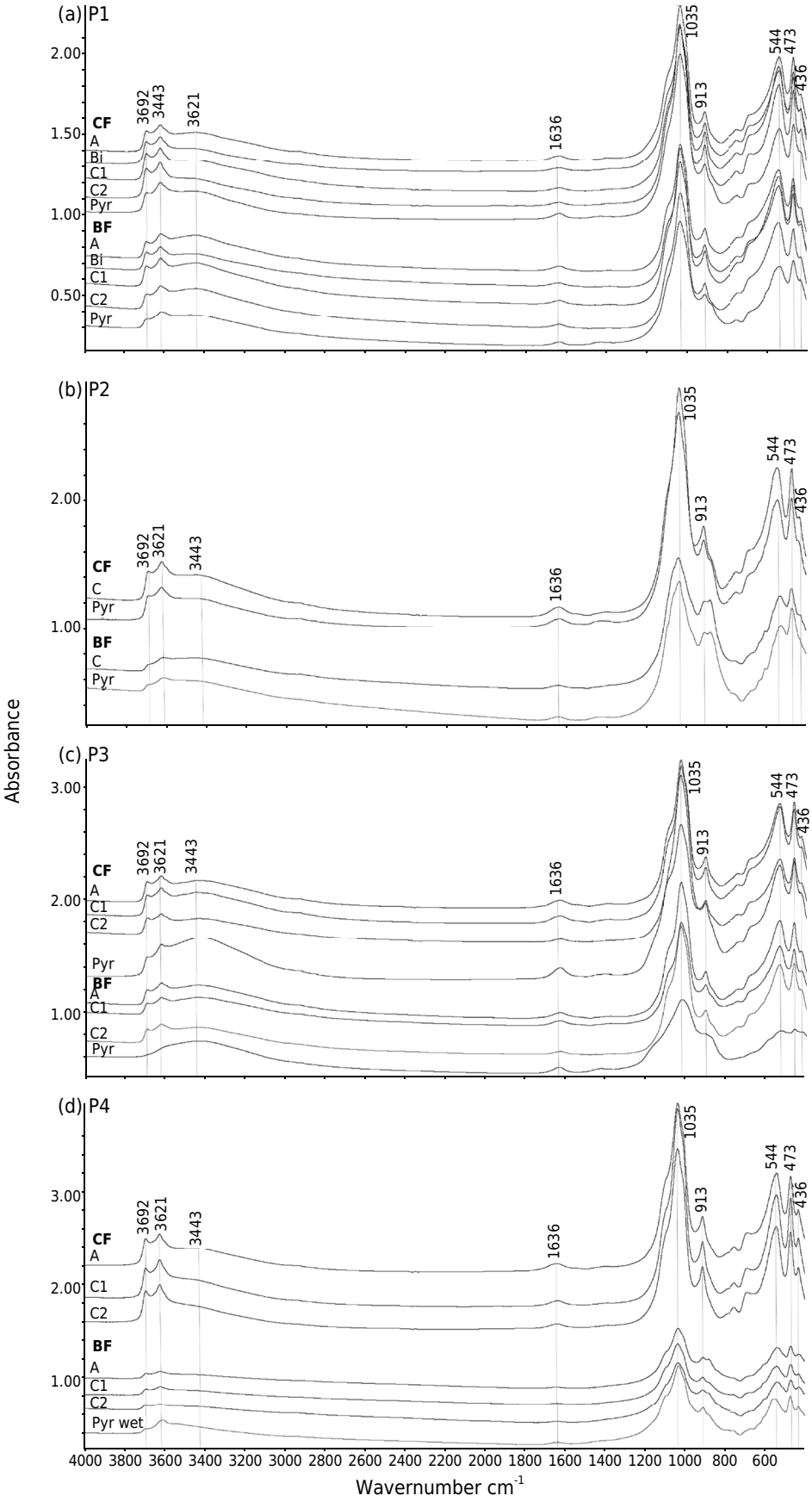

Figure 6. Medium infrared images of pedological horizons of P1 (a), P2 (b), P3 (c), and P4 (d) showing the spectrum of halloysite. In P3 is noted the presence of piques of material non-crystalline in the region between 400 cm^{-1} and 950 cm^{-1}. CF: clay fraction; BF: bulk fraction; Pyr: pyroclast.

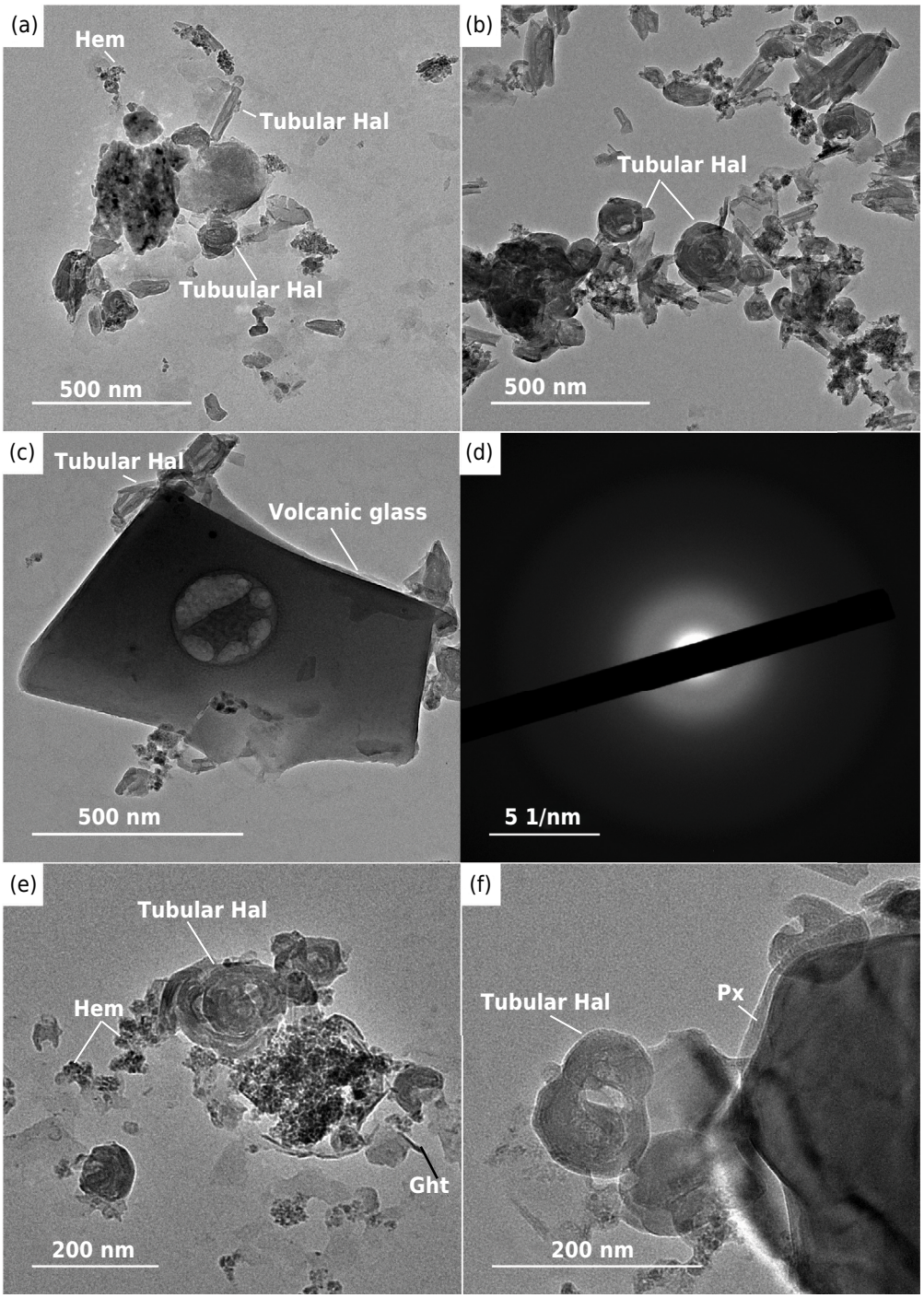

Figure 7. Transmission Electron Microscope images of fraction clay of P1. Tubular halloysite and iron oxides (hematite) in pyroclast (a). Tubular halloysite in C2 horizon (b). It is noted that the halloysite are very crystallized. Volcanic glass and halloysite in C2 horizon (c). Microdiffraction with a characteristic of amorphous material (d). Tubular halloysite iron oxyhydroxides (globular hematite and acicular goethite) in Bi horizon (e). Tubular halloysite near to the crystal pyroxene in A horizon (f). Hal: halloysite; Hem: hematite; Ght: goethite; Px: pyroxene.

size, subhedral magnetite of 0.1 mm size, and altered olivines of 2.0 mm size occur, respectively, in sizes of 5.0, 0.03, and 1.0 mm at the top (A horizon) of the profile.

Aggregates occur in Bi and A horizons and show undifferentiated b-fabric micromass (Figure 3i). As pedological features, reddish and yellowish clay coatings occur, evidencing illuviation of fine colloidal materials (Figures 3e and 3f) and infillings of clay due to the bioturbation (Figure 3i).

DISCUSSION

The presence of andic properties on TI soils was evaluated using the criteria in the Soil Taxonomy (Soil Survey Staff, 2014), for moderate or weakly weathered soils, and in the IUSS Working Group WRB (2015). Recently, in 2018, the Brazilian Soil Classification System – SiBCS (Santos et al., 2018) incorporated this property, using the same criteria used by the IUSS Working Group WRB (2015) (Table 5).

According to Soil Survey Staff (2014), soil with andic properties must have less than 25 % of total organic carbon (TOC), with one of the following criteria that must be met: 1) for moderately weathered soil: the values of [Al(o) + ½Fe(o)] >2 %; the bulk density of soil equal or minor than 0.90 g cm^{-3} and phosphate retention equal or minor than 85 %; or 2) for weakly weathered soil: ratio [Al(o)+ ½Fe(o)] ≥0.4 %; phosphate retention ≥25 %; 30 % or more of sand and silt particles; volcanic glass content ≥5 % and [(Al(o) +½ Fe(o)].(15.625) + (volcanic glass content in %) ≥36.25. In addition, the andic properties quoted in criteria 1 or 2 should occur 60 % of the soil profile. For IUSS Working Group WRB (2015) and SiBCS (Santos et al., 2018), only the parameters shown in 1 are taken into account.

Considering the Soil Taxonomy criteria 1, WRB and SiBCS, only three horizons (P1A, P1C2, and P3A) met all criteria. The main attribute not met was the bulk density, since only the A horizons of P1, P3, and P4, and C2 horizon of P1 showed density lower than 9.00 × 10^7 mg m^{-3}. However, except for the P4C1 horizon (Table 2), the values are not much greater than 9.00 × 10^7 mg m^{-3}, varying between 9.30 × 10^7 and 10.00 × 10^7 mg m^{-3}, so very close to the limit.

The soils of TI have met criterion 2 of the Soil Survey Staff (2014) because they contain less than 25 % of TOC (Table 2) and are weakly weathered. The presence of primary minerals in A and B horizons (glass, olivine, pyroxenes, and feldspar), inside and outside of altered pyroclast fragments, including in the clay fraction, corroborate the low weathering degree of these soils (Figures 3d, 3e, and 3i). The P1, P2, and P3 have andic properties by this criterion in 60 % of their profiles (Table 5). Only the Bi horizon of P1 showed a value lower than of the sum [(Al (O) + 1/2 Fe (o)] × 15.625 + volcanic glass content (%) ≥36.25, while the C2 horizon of P3 presented less than 5 % of volcanic glass, and

Table 5. Diagnostic criteria to andic properties according to (I) Soil Taxonomy (Soil Survey Staff, 2014) for moderately weathered soils, IUSS Working Group WRB (2015), and SiBCS (Santos et al., 2018), and (II) Soil Taxonomy for weakly weathered soils

Pedon	Hor.	I			AP	II						AP
		A ≥2	BD ≤0.9	PR ≥85		TOC <25	A ≥0.4	PR ≥ 5	sand and silt ≥30	VG ≥5	B	
		%	Mg m^{-3}	%		%						
P1	A	2.20	7.5*10^7	96.33	*	0.00	2.20	96.33	52.1	5.4	39.77	*
	Bi[1]/Bw[2]	1.80	9.3*10^7	95.66		1.45	1.80	95.66	45.0	5.0	33.12	
	C1	2.23	9.3*10^7	95.66		2.15	2.23	95.66	58.1	7.4	42.24	*
	C2	2.00	7.1*10^7	93.66	*	0.00	2.00	93.66	60.6	12.76	44.24	*
P2	C	1.85	11.6*10^7	66.55		7.19	1.85	66.55	59.2	8.1	37.01	*
P3	A	2.13	7.2*10^7	85.16	*	18.03	2.13	85.16	42.6	20.96	54.24	*
	C1	2.50	10.1*10^7	87.00		12.99	2.50	87.00	42.3	16.66	55.72	*
	C2	2.06	9.6*10^7	89.16		0.69	2.06	89.16	31.9	3.5	35.69	
P4	A	2.21	7.1*10^7	68.00		9.39	2.21	68.00	68.3	5.9	40.43	*
	C1	2.17	13.8*10^7	64.66		2.15	2.17	64.66	73.7	0.59	34.50	
	C2	1.95	-	65.66		2.15	1.95	65.66	79.2	0.63	31.10	

Hor.: horizon; TOC: total organic carbon (Yeomans and Bremner, 1988); PR: phosphate retention (Alvarez et al., 2000); A = (Al(o) +½ Fe(o); B = [(Al(o) +½ Fe(o)]×(15.625) + (volcanic glass content, percent) ≥36.25; AP: andic properties; * horizon with all criteria met. [1] Coding of horizon according to Brazilian Soil Classification System (Santos et al., 2018). [2] Coding of horizon according to Soil Taxonomy (Soil Survey Staff, 2014).

therefore only, these two horizons do not follow criterion 2. The P4 soil did not have 5 % volcanic glass in 60 % of the profile, and therefore does not meet criterion 2, either (Table 5). It is important to emphasize that the C2 horizon of P4 consists of fragments of a mineralogical composition different from the other profiles, suggesting a different volcanic event of pyroclastic bomb deposition.

In addition, based on criterion 2, the andic properties detected were: ratio Al(o) + ½Fe(o) higher than 0.4 % (Table 5); phosphate retention (PR) greater than 25 % in all horizons, with values between 65 and 97 % (Table 2); the sand and silt contents exceeding 30 % in all profiles (Table 1), corroborating less weathered soils; also, all horizons, excluding the C2 and C1 of P4 and C2 of P3, showed at least 5 % of glass volcanic in the coarse sand fraction in part of the profile (Table 1; Figure 2).

Pyroclasts fragments consisting of palagonized glass corroborate the content of more than 5 % of volcanic glass in the 2 mm fraction (Figures 3b, 3d, 3g, and 3h).

The NaF values greater than 9.4 also indicate the presence of non-crystalline minerals. However, all profiles presented little amounts of allophane (between 0.36 and 3.19 %), and the Si(o) content ≥0.6 % further suggests the presence of these amorphous materials. The pH(H_2O) >5 in all profiles and low content of organic material would contribute to the allophane formation (Dahlgen et al., 1993). The values of the Fe(o)/Fe(d) ratio are also high in all profiles, indicating the presence of no crystalline minerals and a poorly weathered soil (Table 5).

Although the selective extractions indicated the presence of amorphous minerals, the mineralogical analyses (XRD, Infrared, and TEM) could not detect their presence, although halloysite was found. Consistently, in Cabo Verde Island, halloysitic soils with high amounts Al–humus complexes were classified as non-allophanic Andosols (Madeira et al., 1994). Accordingly, soils of the present study have an undifferentiated b-fabric characteristic of the gradual replacement of allophane by halloysite, and illuviation features in all horizons, particularly more pronounced in the Bi horizon of P1, shows that they are Andosols intermediate to soils with more crystalline clays (Stoops et al., 2018).

The classification of non-allophanic horizons requires some properties, such as Alp/Alo of 0.5 or more, and/or Si(o) content of less than 6 g kg^{-1}; and thickness of 0.25 m or more (Tamura, 2012; USCS, 2002). All profiles of this study have Si(o) content less than 6 g kg^{-1} and thickness of 0.25 m or more, so, they can be classified as non-allophanic Andosols. Alternative names for allophane-like materials which could be used are defective kaolin allophane or halloysite-like allophane, when Al:Si ratio value is near 1 (Yoshinaga, 1986) or proto-imogolite allophane and imogolite-like, when this ratio is between 2 and 4 (Farmer and Fraser, 1979; Parfitt and Wilson, 1985). In this case, the soils of P1 and P3 would present halloysite-like allophane, whereas P4 a proto-imogolite allophane and imogolite-like. According to the IUSS Working Group WRB (2015) soils in which allophane, imogolite and similar minerals are predominant, have silandic properties [Si(o) content of ≥0.6 % or an Al(p)/Al(o) of <0.5].

We suggest that sideromelane is the likely precursor of halloysite in TI soils. The study of Mateus et al. (2020) on the alteration of pyroclasts of TI showed the presence of little quantities of halloysite in zones where occur altered sideromelane (palagonite) occurs. In addition, the halloysite of P4 also has feldspars as possible precursors (oligoclase and anorthoclase), besides volcanic glass.

Soils with andic properties, also considered non-allophanic, have already been recognized in the Brazilian territory. In a pioneer report, Ker (1988) suggested the possibility of soils with andic properties in southern Brazil. Later, Gama et al. (1992) also suggested that soils from Acre State could have this character. None of the above studies have demonstrated allophanic soils, and only Dümig et al. (2008) effectively reported the first Andosols of Brazil, identified in the northeast plateau of the Rio Grande do Sul State.

From this study, IUSS Working Group WRB (2015) began to recognize Andosols originated from non-volcaniclastic parent materials in humid regions.

Recently, Santos Junior (2017) confirmed the presence of non-allophanic Andosols in the escarpment of Serra Geral Formation, in the states of Santa Catarina and Rio Grande do Sul. This author identified eight Aluandic Andosols, and two Histosols with andic properties. The organometallic complexes formed in the cold-humid-high elevation areas explained the formation of soils with andic properties associated with non-volcanoclastic rocks.

Trindade Island soils show an unusual situation, with non-allophanic soils derived from typic pyroclastic materials. As previously described, the other non-allophanic soils in Brazil occur because of cold climate conditions and the role of the organic matter. Sieffermann and Millot (1969) studied the soil genesis on Late Quaternary pyroclastic rocks, scorias, tuffs, and ashes of basaltic composition from the Federal Republic of Cameroon. Sieffermann and Millot (1969) showed that in tropical climates, with average annual precipitation between 1.5 and 1.6 m, and a marked dry season and in less leached zones, there is a rapid neoformation of halloysite through allophane as an intermediate phase, maintaining lower amounts of allophane. In our study at TI, we have found similar characteristics: pyroclasts of basaltic composition and tropical oceanic climate with average annual rainfall between 926 mm and a marked dry season, between January and March. Therefore, the climatic conditions of the island could contribute to the rapid formation of halloysite from an allophane precursor, helping to explain the small amounts of allophane in these soils.

Andosols show a well-developed medium granular microstructure at the top which changes to coalesced microstructures towards the bottom of profile (Sedov et al., 2010), very similar to those reported here, but less stable than microgranular microstructures of *Latossolos* (Oxisols). The A horizons showed a granular microstructure, with an undifferentiated b-fabric typical of Andosols on pyroclasts from oceanic islands Pico and Fail in Azores (Gérard, 2007), Terceira (Pinheiro et al., 2003), Canarias (Sanchez Diaz, 1978; Benayas et al., 1980), and Santa Fé (Morrás, 1978).

Despite the criteria of the IUSS Working Group WRB (2015) be considered satisfactory for the SiBCS (Santos et al., 2018), they fail to meet the specificities of TI soils. Soil Taxonomy will offer better conditions to incorporate soils with andic properties with different degrees of development. Thus, we believe that the criteria currently adopted by Soil Survey Staff (2014) are more adequate for keying out soils like those of Trindade Island, in the SiBCS.

There is no place for Andosols in the SiBCS. Using the current system (Santos et al., 2018), the soils of this study would be classified as *Cambissolo Háplico Sódico típico* (P1), with A moderate, presence of Bi horizon, and lower base saturation (<50 %) (Table 2); *Neossolo Regolítico Eutrófico típico* (P3), and *Neossolo Regolítico Eutrófico solódico* (P4). The P3 has A moderate, absence of B, lithic contact at a depth greater than 0.50 m, with semi-altered pyroclasts fragments within the C; P4 is different from P3 because it presents a solodic character (sodium saturation between 6 and 15 % in C2 horizon) (Table 2).

Table 6. Classification of TI soils according to SiBCS (2018), IUSS Working Group WRB (2015), and Soil Taxonomy (Soil Survey Staff, 2014), respectively

Pedon	SiBCS	WRB	ST
P1	*Cambissolo Háplico Sódico Típico*	Vitric Aluandic Andosol	Alic Hapludand
P2	*Neossolo Regolítico Eutrófico típico*	Eutric Leptic Regosol	Typic Hapludand
P3	*Neossolo Regolítico Eutrófico típico*	Eutric Leptic Regosol	Typic Hapludand
P4	*Neossolo Regolítico Eutrófico solódico*	Sodic Eutric Leptic Regosol	Typic Udipsamments

Using the IUSS Working Group WRB (2015), only pedon (P1) can be classified as Andosol (Table 6). The others are classified as Regosols, but this class does not admit the andic suffixes as supplementary qualifiers. The reason why some pedons, such as P3, have not been classified as Andosols is because even though they have the andic properties on the A horizon, they are 0.20 m thick, whereas a minimum of 0.30 m is required by the WRB/FAO System. According to Soil Survey Staff (2014), P1, P2, and P3 are all Andisols, respectively Alic and Typic Hapludand.

We recommend two possibilities to improve the SiBCS in view of the presence of Andosols in TI: 1) the expansion of research in other regions of Brazil, such as in Brazilian oceanic islands and in places where occur similar pedoenvironmental characteristics found in these islands for inclusion of the Andosols order in the SiBCS and/or; 2) the adoption of Soil Taxonomy criteria for the definition of andic properties for weakly weathered soils, maintaining the WRB/FAO criteria already included in 2018.

CONCLUSIONS

The soils of Trindade Island (TI) present andic properties and should be classified as Andosols, and meeting the criteria to be classified as non-allophanic Andosols. In addition, the micromorphological features are like the Andosols described from elsewhere.

The Andosols in TI are non-allophanic for a different reason, compared with other non-allophanic Andosols already reported in Brazil. In Trindade Island, soils are derived from pyroclastic materials, and the silandic conditions are weakened by the rapid weathering under warmer climates. Other non-allophanic soils in the southern highlands of Brazil have andic properties because were formed under cold-mesothermic climate conditions.

The predominance of halloysite in the clay fraction is consistent with the non-allophanic character of TI soils. Halloysite was formed by alteration of sideromelane, in which allophane is the intermediate phase.

These unique TI soils should be recognized in the SiBCS as special soils, and the adoption of Soil Taxonomy criteria for weakly weathered soils allows us to classify them out as non-allophanic Andosols.

ACKNOWLEDGMENTS

Special thanks to the Brazilian Navy for their logistical support and to the CNPq (306424/2016-9; 442730/2015-2), CAPES (Finance code 001), and FAPEMIG (PPM-00326-18) for their financial contribution. We would also like to express our gratitude to the Microanalysis Laboratory of the Universidade Federal de Ouro Preto, member of the Microscopy and Microanalysis Network of Minas Gerais State/Brazil/FAPEMIG and to the Laboratory of Microanalysis Netwirk of Minas Gerais State/Brazil/FAPEMIG and to the Laboratory of Microanalysis and Eletronic Microscopy Center of the Universidade Federal de Minas Gerais for the mineral chemical analyses. Lastly, we would like to show our appreciation to the Laboratory of X-Ray Difraction of DEGEO/UFOP DRX and laboratory IC2MP, Université de Poitiers for the mineralogical analyses. Authors also acknowledged financial support from the European Union (ERDF) and Région Nouvelle Aquitaine; and CINam-CNRS in the Aix Marseille University by TEM analysis.

AUTHOR CONTRIBUTIONS

Conceptualization: Ana Carolina Campos Mateus (equal), Angélica Fortes Drummond Chicarino Varajão (equal), Fábio Soares de Oliveira (equal), and Sabine Petit (equal).

Methodology: Ana Carolina Campos Mateus (equal), Angélica Fortes Drummond Chicarino Varajão (equal), Fábio Soares de Oliveira (equal), and Sabine Petit (equal).

Software: Ana Carolina Campos Mateus (lead).

Validation: Ana Carolina Campos Mateus (lead).

Formal analysis: Ana Carolina Campos Mateus (lead).

Investigation: Ana Carolina Campos Mateus (equal), Carlos Ernesto Gonçalves Reynaud Schaefer (equal), Angélica Fortes Drummond Chicarino Varajão (equal), Fábio Soares de Oliveira (equal), and Sabine Petit (equal).

Resources: Carlos Ernesto Gonçalves Reynaud Schaefer (equal), Angélica Fortes Drummond Chicarino Varajão (equal), Fábio Soares de Oliveira (equal), and Sabine Petit (equal).

Data curation: Angélica Fortes Drummond Chicarino Varajão (equal) and Sabine Petit (equal).

Writing – original draft: Ana Carolina Campos Mateus (lead).

Writing – review and editing: Carlos Ernesto Gonçalves Reynaud Schaefer (equal), Angélica Fortes Drummond Chicarino Varajão (equal), Fábio Soares de Oliveira (equal), and Sabine Petit (equal).

Visualization: Ana Carolina Campos Mateus (equal), Angélica Fortes Drummond Chicarino Varajão (equal), Fábio Soares de Oliveira (equal), and Sabine Petit (equal).

Supervision: Angélica Fortes Drummond Chicarino Varajão (equal), Fábio Soares de Oliveira (equal), and Sabine Petit (equal).

Project administration: Carlos Ernesto Gonçalves Reynaud Schaefer (equal), Angélica Fortes Drummond Chicarino Varajão (equal), and Fábio Soares de Oliveira (equal).

Funding acquisition: Carlos Ernesto Gonçalves Reynaud Schaefer (equal), Angélica Fortes Drummond Chicarino Varajão (equal), Fábio Soares de Oliveira (equal), and Sabine Petit (equal).

REFERENCES

Adjadeh TA, Inoue K. Andisols of the Kitakami mountain range, Northeastern Japan: their characterization and classification. Soil Sci Plant Nutr. 1999;45:115-30. https://doi.org/10.1080/00380768.1999.10409328

Almeida BG, Viana JHM, Teixeira WG, Donagema GK. Densidade do solo. In: Teixeira PC, Donagemma GK, Fontana A, Teixeira WG. Manual de métodos de análise de solo. 3. ed. rev e ampl. Brasília, DF: Embrapa; 2017. p. 65-7.

Almeida FFM. Ilhas oceânicas brasileiras e sua relação com a tectônica atlântica. Terræ Didatica. 2006;2:3-18. https://doi.org/10.20396/td.v2i1.8637462

Almeida FFM. Ilha de Trindade - registro de vulcanismo cenozoico no Atlântico Sul. In: Schobbenhaus C, Campos DA, Queiroz ET, Winge M, Berbet-Born MLC, editores. Sítios geológicos e paleontológicos do Brasil. Brasília: DNPM/CPRM - Comissão Brasileira de Sítios Geológicos e Paleobiológicos (SIGEP); 2002. p. 369-77.

Alvarez V VH, Novais RF, Dias LE, Oliveira JA. Determinação e uso do fósforo remanescente. Boletim Informativo da Sociedade Brasileira de Ciência do Solo. 2000;25:27-32.

Bech-Borras J, Fedoroff N, Sole A. Etude des andosols d'Olot (Gerona, Espagne). 3 partie: Micromorphologie. Cah Orstom Ser Pedol. 1977;15:381-90.

Benayas J, Fernandez-Caldas E, Tejedor Salguero ML, Rodriguez-Rodriguez A. Caracteristicas micromorphologicas de los suelos de un clima secuencia de la vertiente meridional de la Isla de Tenerife. Anales de Edafología y Agrobiología. 1980;3:51-74.

Bertrand S, Fagell N. Nature and deposition of andosol parent material in south-central Chili (36-42 °C). Catena. 2008;73:10-22. https://doi.org/10.1016/j.catena.2007.08.003

Blakemore LC, Searle PL, Daly BK. Methods for chemical analysis of soils. New Zealand: Csiro; 1981. (New Zealand Soil Bureau Sc1entif1c Report 10A).

Brown G, Brindley GW. Crystal structures of clay minerals and their X-ray identification. London: Mineralogical Society; 1980.

Brydon JE, Day JH. Use of the Fieldes and Perrott sodium fluoride test to distinguish the B horizons of Podzols in the field. Can J Soil Sci. 1970;50:35-41. https://doi.org/10.4141/cjss70-005

Candan F, Broquen P. Aggregate stability and related properties in NW Patagonian Andisols. Geoderma. 2009;154:42-7. https://doi.org/10.1016/j.geoderma.2009.09.010

Caner L, Bourgeon G, Toutain F, Herbillon AJ. Characteristics of non-allophanic Andisols derived from low-activity clay regoliths in the Nilgiri Hills (Southern India). Eur J Soil Sci. 2000;51:553-63. https://doi.org/10.1111/j.1365-2389.2000.00344.x

Clemente EP. Ambientes terrestres da Ilha da Trindade, Atlântico Sul: caracterização do solo e do meio físico como subsídio para criação de uma unidade de conservação [tese]. Viçosa, MG: Universidade Federal de Viçosa; 2006.

Clemente EP, Schaefer CE, Oliveira FS, Albuquerque-Filho MR, Alves RV, Sá MMF, Melo VS. Topossequência de solos na Ilha da Trindade, Atlântico Sul. Rev Bras Cienc Solo. 2009;33:1357-71. https://doi.org/10.1590/S0100-06832009000500028

Dahlgren R, Shoji S, Nanzyo M. Mineralogical characteristics of volcanic ash soils. In: Shoji S, Nanzyo M, Dahlgren R, editors. Volcanic ash soils: genesis, properties and utilization. Amsterdam: The Netherlands; 1993. p. 101-43.

Defelipo BV, Ribeiro AC. Análise química do solo (metodologia). Viçosa, MG: Universidade Federal de Viçosa; 1981. (Boletim de extensão 29).

Devnita R. Melanic and Fulvic Andisols in Volcanic Soils derived from some Volcanoes in West Java. Indonesian Journal of Geology. 2012;7:227-40. https://doi.org/10.17014/ijog.7.4.227–240

Deer WA, Howie RA, Zussman J. An Introduction to the Rock-Forming Minerals. Great Britain and Ireland: Mineralogical Society. 2013. https://doi.org/10.1180/DHZ

Diniz AC, Matos GC. Carta de zonagem agro-ecológica e da vegetação de Cabo Verde. V - Ilha do Sal. Garcia de Orta - Ser Bot. 1993;11:9-30.

Diniz AC, Matos GC. Carta de zonagem agro-ecológica e da vegetação de Cabo Verde. VI - Ilha de S. Vicente. Garcia de Orta - Ser Bot. 1994a;12:69-98.

Diniz AC, Matos GC. Carta de zonagem agro-ecológica e da vegetação de Cabo Verde. VIII - Ilha de S. Nicolau. Garcia de Orta - Ser Bot. 1999a;14:1-54.

Diniz AC, Matos GC. Carta de zonagem agro-ecológica e da vegetação de Cabo Verde. IX - Ilha Brava. Garcia de Orta - Ser Bot. 1999b;14:55-82.

Dümig A, Schad P, Kohok M, Beyerlein P, Schwimmer W, Kögel-Knabner I. A mosaic of nonallophanic Andosols, Umbrisols and Cambisols on rhyodacite in the southern Brazilian highlands. Geoderma. 2008;145:158-73. https://doi.org/10.1016/j.geoderma.2008.01.013

Eguchi T, Tamura K. Characterization of Andosols in Yakushima Island. Soil Sci Plant Nutr. 2012;58:52-64. https://doi.org/10.1080/00380768.2011.653691

Espinosa JAS, Sanabria YR. Procesos específicos de formación en Andisoles, Alfisoles y Ultisoles en Colombia. Rev EIA. 2015;12:85-97. https://doi.org/10.14508/reia.2015.11.E2.85-97

Faria FX. Os solos da Ilha do Fogo (arquipélago de Cabo Verde). Lisboa: Junta de Investigações Científicas do Ultramar; 1974. (Estudos, Ensaios e Documentos nº 129).

Farmer VV, Fraser AR. Synthetic imogolite, a tubular hydroxy-aluminium silicate. In: Mortland MM, Farmer VC, editors. International Clay Conference 1978. Amsterdam: Elsevier; 1979. p. 547-53.

Fernandez-Calilas E, Tejedors U, Guero ML. Andosoles de las Islas Canarias. Tenarife: Servicio de Publicacione de la Caja General de Ahorros de Santa Cruz; 1975.

Fields M, Perrot KW. The nature of allophane in soils. III. Gypsum effects on growth and subsoil chemical proprieties. Soil Sci Soc Am J. 1966;2:623-9.

Gama JRNF, Kusuba T, Ota T, Amano Y. Influência de material vulcânico em alguns solos do estado do Acre. Rev Bras Cienc Solo. 1992;16:103-6.

Garcia-Rodeja E, Silva BM, Macías F. Andosols developed from non-volcanic materials in Galicia, NW Spain. J Soil Sci. 1987;38:573-91. https://doi.org/10.1111/j.1365-2389.1987.tb02156.x

Gérard M, Caquineau S, Pinheiro J, Stoops G. Weathering and allophane neoformation in soils developed on volcanic ash in the Azores. Eur J Soil Sci. 2007;58:496-515. https://doi.org/10.1111/j.1365-2389.2007.00910.x

Grison H, Petrovsky E, Stejskalova S, Kapicka A. Magnetic and geochemical characterization of Andosols developed on basalts in the Massif Central, France. Geochem Geophys Geosyst. 2015;16:1348-63. https://doi.org/10.1002/2015GC005716

Hikmatullah. Andisols from Tondano Area, North Sulawesi: properties and classification. Jurnal Tanah Tropika. 2008;13:77-85.

Holmgreen GGS. A rapid citrate-dithionite extractable iron procedure. Soil Sci Soc Am Proc. 1967;31:210-1. https://doi.org/10.2136/sssaj1967.03615995003100020020x

IUSS Working Group WRB. World reference base for soil resources 2014, update 2015: International soil classification system for naming soils and creating legends for soil maps. Rome: Food and Agriculture Organization of the United Nations; 2015. (World Soil Resources Reports, 106).

Ker JC. Caracterização química, física, mineralógica e micromorfológica de Solos Brunos Subtropicais [dissertação]. Viçosa, MG: Universidade Federal de Viçosa; 1988.

Kiliç K, Yalçinb H, Durakc A, Doğand HM. Andisols of Turkey: an example from the Cappadocian Volcanic Province. Geoderma. 2018;313:112-25. https://doi.org/10.1016/j.geoderma.2017.10.019

Litvinenko YS, Zakharikhina LV. Zoning and geochemical characterization of volcanic soils on Kamchatka. Geochem Int. 2009;47:463-75. https://doi.org/10.1134/S0016702909050036

Machado MR. O papel da avifauna na transformação geoquímica de substratos na Ilha da Trindade, Atlântico Sul [dissertação]. Belo Horizonte: Universidade Federal de Minas Gerais; 2016.

MacKeague JA, Day JH. Dithionite and oxalate extractable Fe and Al as aids in differentiating various classes of soils. Can J Soil Sci. 1966;46:13-22. https://doi.org/10.4141/cjss66-003

Madeira M. Esboço pedológico da Ilha de Santa Maria (Açores). Lisboa: Instituto Nacional de Investigação Cientifica Tropical; 1980.

Madeira M, Furtado AFS, Jeanroy E, Herbillon AJ. Andisols of Madeira Island (Portugal). Characteristics and classification. Geoderma. 1994;62:363-83. https://doi.org/10.1016/0016-7061(94)90099-X

Madeira M, Pinheiro J, Medina J. Características físico-químicas e mineralógicas de Andossolos do Arquipélago dos Açores (Portugal) que endurecem irreversivelmente por secagem. In: XIII Congresso Latino-Americano de Ciência do Solo [CD-ROM]; 4-8 de agosto de 1996; Águas de Lindóia (Brasil). Rio de Janeiro: Embrapa; 1996. (Comissão 02, Trabalho 14).

Madruga JS. Características e génese do horizonte plácico em solos do Arquipélago dos Açores [tese]. Angra do Heroísmo: Universidade dos Açores; 1995.

Mateus ACC, Varajão AFDC, Petit S, Oliveira FS, Schaefer CE. Mineralogical and geochemical signatures of Quaternary pyroclasts alterations at the volcanic Trindade Island, South Atlantic. J S Am Earth Sci. 2020;102:1-14. https://doi.org/10.1016/j.jsames.2020.102674

Medina JMB, Grilo JT. Esboço pedológico da Ilha Graciosa (Açores*)*. Lisboa: Instituto Nacional de Investigação Cientifica Tropical e Universidade dos Açores; 1981.

Mehra JP, Jackson ML. Iron oxides removal from soils and clays by dithionite-citrate-bicarbonate system buffered with bicarbonate sodium. Clay Clay Miner. 1960;7:317-27. https://doi.org/10.1016/B978-0-08-009235-5.50026-7

Morrás HJM. Phosphatic nodules from a soil profile of Santa Fé Island, Galapagos. In: Delgado M, editor. Soil micromorphology. Spain: University of Granada; 1978. p. 1007-18.

Munsell AH. Munsell soil color charts. Rev ed. Baltimore: Macbeth Division of Kollmorgen Corporation; 2009.

Neall VE. Genesis and weathering of Andosols in Taranaki. Soil Sci. 1977;123:400-8.

Pansu M, Gautheyrou J. Handbook of soil analysis mineralogical, organic, and inorganic methods. Berlin: Springer; 2006.

Parfitt RL. Allophane in New Zealand - a review. Aust J Soil Res. 1990;28:343-60. https://doi.org/10.1071/SR9900343

Parfitt RL, Childs CW. Estimation of forms of Fe and Al - a review, and analysis of contrasting soils by dissolution and Mossbauer methods. Aust J Soil Res. 1988;26:121-44. https://doi.org/10.1071/SR9880121

Parfitt RL, Wilson AD. Estimation of allophane and halloysite in three sequences of volcanic soils, New Zealand. Catena Supp. 1985;7:1-8.

Pinheiro J. Estudo dos principais tipos de solos da Ilha Terceira (Açores) [tese]. Angra do Heroísmo: Universidade dos Açores; 1990.

Pinheiro J, Madeira M, Monteiro F, Medina J. Características e classificação dos Andossolos da Ilha do Pico (Arquipélago dos Açores). Rev Ciencs Agrar. 2001;24:48-60.

Pinheiro J, Tejedor Salguero M, Rodriguez-Rodriguez A. Genesis of placic horizons in Andisols from Terceira Island, Azores - Portugal. Catena. 2004;56:85-94. https://doi.org/10.1016/j.catena.2003.10.005

Rennert T, Eusterhues K, Hiradate S, Breitzke H, Buntkowsky G, Totsche KU, Mansfeldt T. Characterisation of Andosols from Laacher See tephra by wet chemical and spectroscopic techniques (FTIR, ^{27}Al-, ^{29}Si-NMR). Chem Geol. 2014;363:13-21. https://doi.org/10.1016/j.chemgeo.2013.10.029

Ricardo RP, Madeira MV, Medina JMB, Marques MM, Furtado AFS. Esboço pedológico da Ilha de S. Miguel (Açores). An Inst Sup Agron. 1977;37:275-385.

Sá MMF. Caracterização ambiental, classificação e mapeamento dos solos da ilha da Trindade, Atlântico Sul [dissertação]. Viçosa, MG: Universidade Federal de Viçosa; 2010.

Santos HG, Jacomine PKT, Anjos LHC, Oliveira VA, Lumbreras JF, Coelho MR, Almeida JA, Araújo Filho JC, Oliveira JB, Cunha TJF. Sistema brasileiro de classificação de solos. 5. ed. rev. ampl. Brasília, DF: Embrapa; 2018.

Santos Junior JB. Solos com propriedades ândicas derivados de litologias da Formação Serra Geral em ambientes altomontanos do sul do Brasil [tese]. Lages: Universidade Estadual de Santa Catarina; 2017.

Santos RD, Santos HG, Ker JC, Anjos LHC, Shimizu SH. Manual de descrição e coleta de solo no campo. Viçosa, MG: Sociedade Brasileira de Ciência do Solo; 2015.

Sanchez DJ, Benayas J, Guerra A. Morphological and micromorphological study of the argillic horizons in the arid and subhumid areas of Gran Canaria (Canary Islands). In: Delgado M, editor. Soil micromorphology. Granada: Department of Edaphology, University of Granada; 1978. p. 1067-92.

Schaefer CEGR, Oliveira FS, Marques FA. Solos das ilhas oceânicas. In: Curi N, Ker JC, Novais RF, Vidal-Torrado P, Schaefer CEGR, editores. Pedologia: solos dos biomas brasileiros. Viçosa, MG: Sociedade Brasileira de Ciência do Solo; 2017. p. 545-97.

Sedov SN, Solleiro-Reboledo E, Gama-Castro JE. Andosol to Luvisol evolution in Central Mexico: timing, mechanisms and environmental setting. Catena. 2003;54:495-513. https://doi.org/10.1016/S0341-8162(03)00123-1

Sedov SN, Stoops G, Shoba S. Regoliths and soils on volcanic ash. In: Stoops G, Marcelino V, Mees F, editors. Interpretation of micromorphological features of soils and regoliths. Amsterdam: Elsevier; 2010. p. 275-303.

Shoji S, Ito T, Saigusa M, Yamada L. Properties of non allophanic Andosols from Japan. Soil Sci. 1985;140:264-77.

Shoji S, Nanzyo M, Dahlgren R. Terminology, concepts and geographic distribution of volcanic ash soils. In: Shoji S, Nanzyo M, Dahlgren R, editors. Volcanic ash soils - genesis, properties and utilization. Amsterdam: Elsevier; 1993. p. 1-5.

Shoji S, Ono T. Physical and chemical properties and clay mineralogy of Andosols from Kitakami, Japan. Soil Sci. 1978;126:297-312.

Sieffermann G, Millot G. Equatorial and tropical weathering of recent basalts from Cameroon: allophanes, halloysite, metahalloysite, kaolinite and gibbsite. In: Heller L, editor. Proceedings of the international clay conference in Tokyo. Jerusalem: Israel Program for Scientific Translations; 1969. p. 417-29.

Soil Survey Staff. Keys to soil taxonomy. 11th ed. Washington, DC: United States Department of Agriculture, Natural Resources Conservation Service; 2010.

Soil Survey Staff. Keys to soil taxonomy. 12th ed. Washington, DC: United States Department of Agriculture, Natural Resources Conservation Service; 2014.

Stoops G. Guidelines for analyses and description of soil and regolith thin sections. Madison: Cambridge University Press; 2003.

Stoops G, Sedov S, Shoba S. Regoliths and soils on volcanic ash. In: Stoops G, Marcelino V, Mees F, editors. Interpretation of micromorphological features of soils and regoliths. 2nd ed. Amsterdam: Elsevier; 2018. p. 721-51.

Teixeira PC, Donagemma GK, Fontana A, Teixeira WG. Manual de métodos de análise de solo. 3. ed. rev e ampl. Brasília, DF: Embrapa; 2017.

Unified Soil Classification System of Japan - USCSJ. The fourth committee for soil classification and nomenclature. 2nd approx. Hakuyusha: Japanese Society of Pedology; 2003.

Urushadze TF, Blum WEH, Sanadze EV, Kvrivishvili TO. Andosols of Georgia. Eurasian Soil Sci. 2011;44:969-75. https://doi.org/10.1134/S106422931109016X

Vingiani S, Buonanno M, Coraggio S, D'antonio A, De Mascellis R, Di Gennaro A, Iamarino M, Langella G, Manna P, Moretti P, Terribile F. Soils of the Aversa plain (southern Italy). J Maps. 2018;14:312-20. https://doi.org/10.1080/17445647.2018.1458338

Vingiani S, Scarciglia F, Mileti FA, Donato P, Terribile F. Occurrence and origin of soils with andic properties in Calabria (southern Italy). Geoderma. 2014;232-234:500-16. https://doi.org/10.1016/j.geoderma.2014.06.001

Yeomans JM, Bremner JC. A rapid and precise method for routine determination of organic carbon in soil. Commun Soil Sci Plant Anal. 1988;19:1467-76. https://doi.org/10.1080/00103628809368027

Yoshinaga N. Mineralogical characteristics - II: Clay minerals. In: Wada K, editor. Ando soils in Japan. Fukuoka-shi: Kyushu University Press; 1986. p. 41-56.